

# ADMS 6 Buildings Validation

## *Snyder Wind Tunnel Experiments*

Cambridge Environmental Research Consultants  
April 2023

### 1 Introduction

Experiments were conducted in a simulated boundary layer representative of rural terrain with a few shrubs and trees in neutral conditions. Vertical profiles of concentration were measured downstream of a rectangular building for various stack heights, emission characteristics and building positions.

The model scale in the wind tunnel was 1/200 of full scale. Full details of the building and source parameters are given in Snyder (1993) [1].

Model runs for comparison with the experimental data have been carried out using ADMS 5.2 (version 5.2.0.0) and ADMS 6.0 (version 6.0.0.1). Section 2 describes the input data used for the model. The results are presented and discussed in Section 3. Section 4 gives some additional information about the calculation of the emission characteristics.

### 2 Input data

#### 2.1 Source parameters and buildings

The wind tunnel experiments consisted of a ‘base case’ and a number of variations in which stack height, diameter and exit velocity and building position were varied. The data used as input to the dispersion models for the base case are given in **Tables 1** and **2**.

In the wind tunnel experiments, a mixture of air and helium was used to simulate a high-temperature emission. The calculation of the equivalent emission and ambient temperatures is given in Section 4.

Centre (m)	Height (m)	Length (m)	Width (m)	Angle (°)
(-25,0)	50	100	40	0

**Table 1** – Building dimensions. The centre is given relative to the source. The angle is the angle between north and the building length measured clockwise from north.

Height (m)	Exit V (m/s)	Exit T (°C)	Diameter (m)	Emission rate (g/s)
75	20	145	6	1

**Table 2** – Source input parameters. T is the temperature, V the velocity.

Details of variations from the base case are given in **Table 3**. For the model runs, all parameters except those in the table were identical to the base case for each experiment.

<b>Experiment number</b>	<b>Variation from base case</b>
3_1	stack height = 12.5 m
3_2	stack height = 50 m
3_3	stack height = 125 m
5_2	centre of building = (-100,0)
5_3	centre of building = (-250,0)
5_4	centre of building = (-375,0)
6_2	building centre = (-17.7,17.7), angle = 135°
6_3	building centre = (0,25), angle = 90°
6_4	building centre = (17.7,-17.7), angle = 45°
6_5	building centre = (25,0), angle = 0°
7_1	exit velocity = 15
7_2	exit velocity = 25
7_3	exit velocity = 40
8_1	stack diameter = 6.68
8_2	stack diameter = 3.34
8_3	stack diameter = 1.67
8_4	stack diameter = 0.1

**Table 3** – Range of input data.

## 2.2 Meteorological data

The meteorological data were the same for all experiments (see **Table 4**). Wind speed was measured at the stack height. Hence in the model runs, the height of the wind speed measurements was set equal to the stack height.

<b>Wind speed (m/s)</b>	13.4
<b>Wind direction (°)</b>	270
<b>Boundary layer height (m)</b>	360
<b>Temperature (°C)</b>	20
<b>1/Monin-Obukhov length (m<sup>-1</sup>)</b>	0
<b>Surface roughness (m)</b>	0.2

**Table 4** – Meteorological data.

## 3 Results

### 3.1 Output

In each case, concentrations were calculated 750 m downstream of the source, at a number of heights corresponding to the receptor heights in the wind tunnel. The heights varied slightly from experiment to experiment. Non-dimensional concentrations  $K$  were then calculated as follows:

$$K = \frac{C U H_b^2}{Q}$$

where  $C$  is concentration ( $\mu\text{g}/\text{m}^3$ ),  $U$  is the wind speed at the stack height (m/s),  $H_b$  is the height of the building (m) and  $Q$  is the emission rate ( $\mu\text{g}/\text{s}$ ).

In analysing the results, data points where the observed or modelled concentration was less than 0.01 were removed. In Section 3.2, results are presented as scatter plots and quantile-quantile plots of model results versus observed data, for each model. Summary statistics of the observed and modelled data are given in Section 3.3. The graphs and statistical analysis have been produced by the Model Evaluation Toolkit v5.2 [2].

### 3.2 Scatter and quantile-quantile plots

**Figure 1** shows scatter plots and quantile-quantile plots of all the results for each model.

The scatter plots were created by plotting each modelled concentration against the corresponding observed value. For all of these plots, concentrations are given as the non-dimensional value multiplied by  $10^3$ . The scatter plots show that the majority of the model predictions are within a factor of two of the observations.

The quantile-quantile plots were created by plotting the highest modelled concentration against the highest observed concentration, the second highest modelled concentration against the second highest observed concentration, and so on.

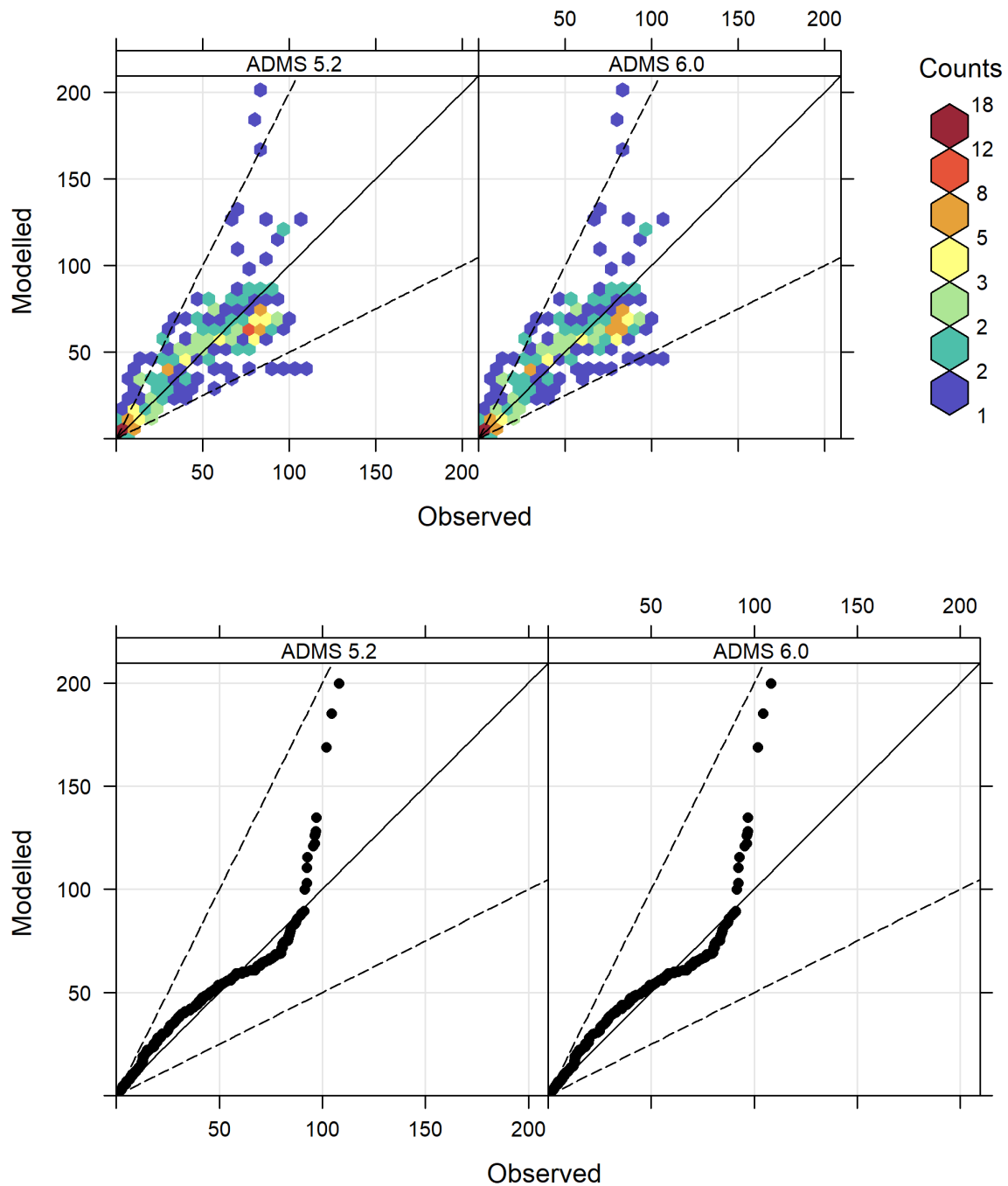


**Figure 1** – Scatter and quantile-quantile plots of each model against observed data. ( $\mu\text{g}/\text{m}^3$ ).

### 3.3 Statistics

The Model Evaluation Toolkit produces statistics of the data that are useful in assessing model performance. Statistics calculated include mean, standard deviation (Sigma), bias, normalised mean square error (NMSE), correlation (Cor), fraction of results where the modelled and observed concentrations agree to within a factor of two (Fa2), fractional bias (Fb) and fractional standard deviation (Fs).

The data were analysed in two ways. Firstly the observed concentrations were compared

directly with the modelled values. The results are shown in **Table 5**.

Data	Mean	Sigma	Bias	NMSE	Cor	Fa2	Fb	Fs
Observed	45.16	31.28	0.00	0.00	1.000	1.000	0.000	0.000
ADMS 5.2	46.95	33.06	1.79	0.19	0.811	0.851	0.039	0.055
ADMS 6.0	47.07	33.09	1.91	0.18	0.818	0.866	0.041	0.056

**Table 5** – Summary statistics comparing observed and modelled concentrations.

This method of analysing the data gives extra weight to the higher concentrations, so that for example, under-predicting the highest concentration by 10 % will have a much larger effect on the standard deviation than under-predicting the lowest concentration by 10 %. Hence the data were also analysed by normalising each concentration by the observed value. The results are shown in **Table 6**.

Data	Mean	Sigma	Bias	NMSE	Fa2	Fb
Observed	1.00	0.00	0.00	0.00	1.000	0.000
ADMS 5.2	1.33	1.42	0.33	1.60	0.854	0.281
ADMS 6.0	1.32	1.42	0.32	1.60	0.869	0.277

**Table 6** – Summary statistics comparing observed and modelled concentrations, normalised by the observed values.

The model has a tendency to predict slightly higher concentrations than those observed, though the correlation is still good ( $>0.8$ ).

The differences between ADMS 5.2 and ADMS 6.0 are generally small. For the non-normalised concentrations, ADMS 6.0 performs slightly better than ADMS 5.2 in terms of NMSE, correlation and Fa2 but slightly worse in terms of mean concentration, sigma, bias, Fb and Fs. For the normalised concentrations, ADMS 6.0 performs the same as or slightly better than ADMS 5.2 across all statistics presented. In ADMS 6.0, the ground-level plume emanating from recirculation region is modelled as a line source rather than a point source, with an initial concentration that is better matched to the uniform concentration of the entrained part of the plume within the well-mixed recirculation region; this is affecting results slightly. The new model development relating to how plumes that directly impact a building are modelled does not affect this study as there are no configurations in this study where the source is both upwind, and below the roof height, of the building.

The Model Evaluation Toolkit was also used to produce box and whisker plots to assess how model performance varies as each input parameter varies. The 5<sup>th</sup>, 25<sup>th</sup>, 50<sup>th</sup>, 75<sup>th</sup> and 95<sup>th</sup> percentile concentrations for each value of each input parameter were calculated. **Figures 2 to 6** illustrate the variation with stack height, stack diameter, stack exit velocity, upstream position of building relative to the source, and position and orientation of the building.

Figures 2 to 6 show that the performance of ADMS is fairly uniform over the whole range of parameters studied. The differences between ADMS 5.2 and ADMS 6.0 are small. The most noticeable difference is for the case with the lowest stack height, where ADMS 6.0 concentrations are closer to observed. A lower source will have a larger entrained fraction within the recirculation region and thus the ground-level plume change will have a larger effect.

**Box and Whisker Plot: 5.2 VS 6.0, ALL STATIONS, HOURLY MEAN SO<sub>2</sub>**

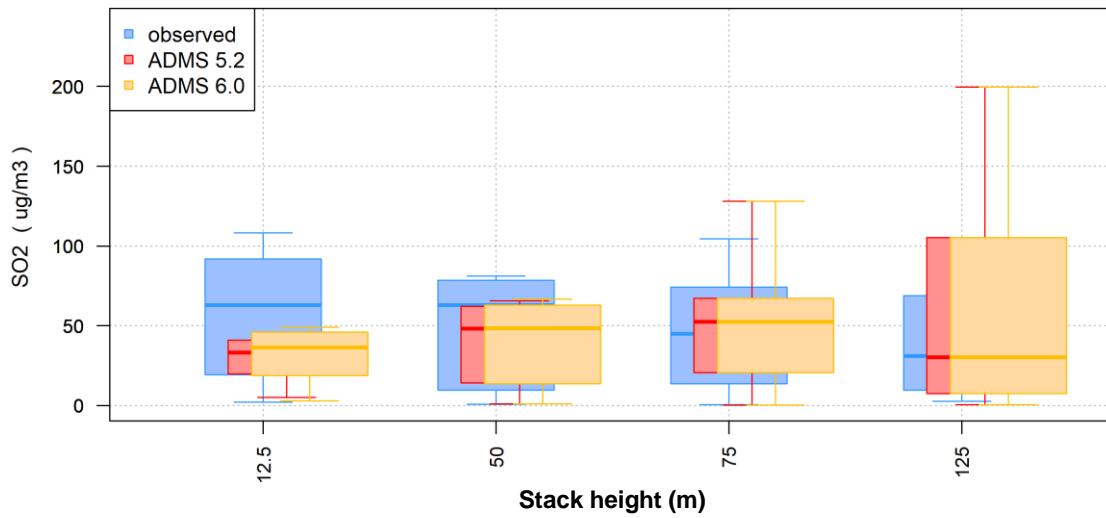


**Figure 2** – Box and whisker plot of model results, variation with stack height.

**Box and Whisker Plot: 5.2 VS 6.0, ALL STATIONS, HOURLY MEAN SO<sub>2</sub>**

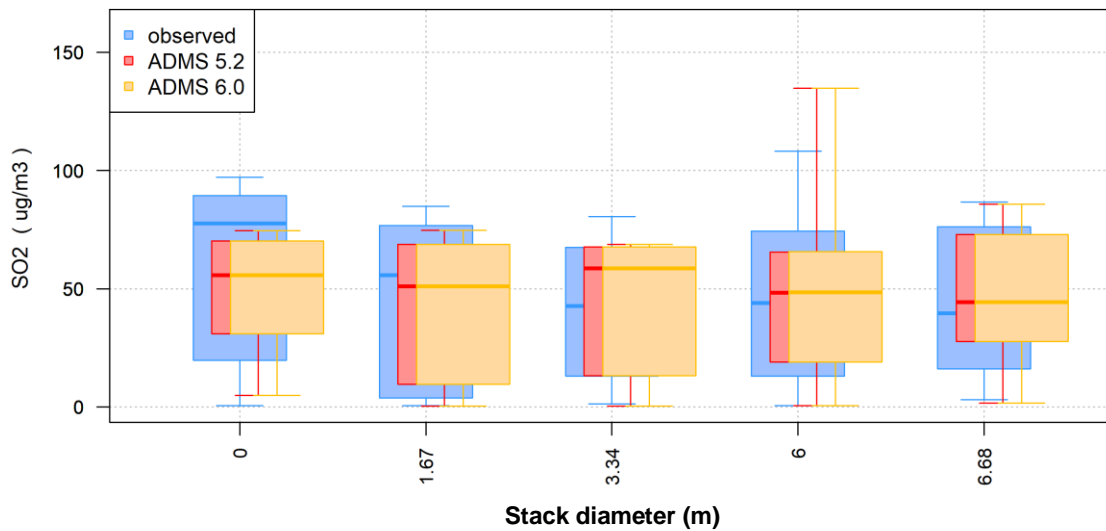


**Figure 3** – Box and whisker plot of model results, variation with stack diameter.

**Box and Whisker Plot: 5.2 VS 6.0, ALL STATIONS, HOURLY MEAN SO<sub>2</sub>**

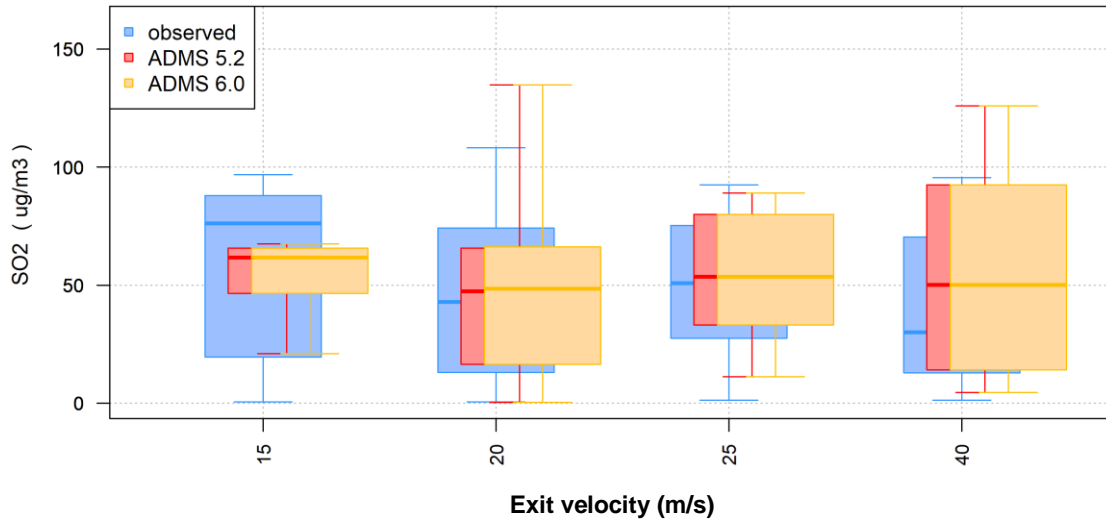


**Figure 4 – Box and whisker plot of model results, variation with exit velocity.**

**Box and Whisker Plot: 5.2 VS 6.0, ALL STATIONS, HOURLY MEAN SO<sub>2</sub>**



**Figure 5 – Box and whisker plot of model results, variation with x-coordinate of building centre relative to source (y-coordinate = 0).**

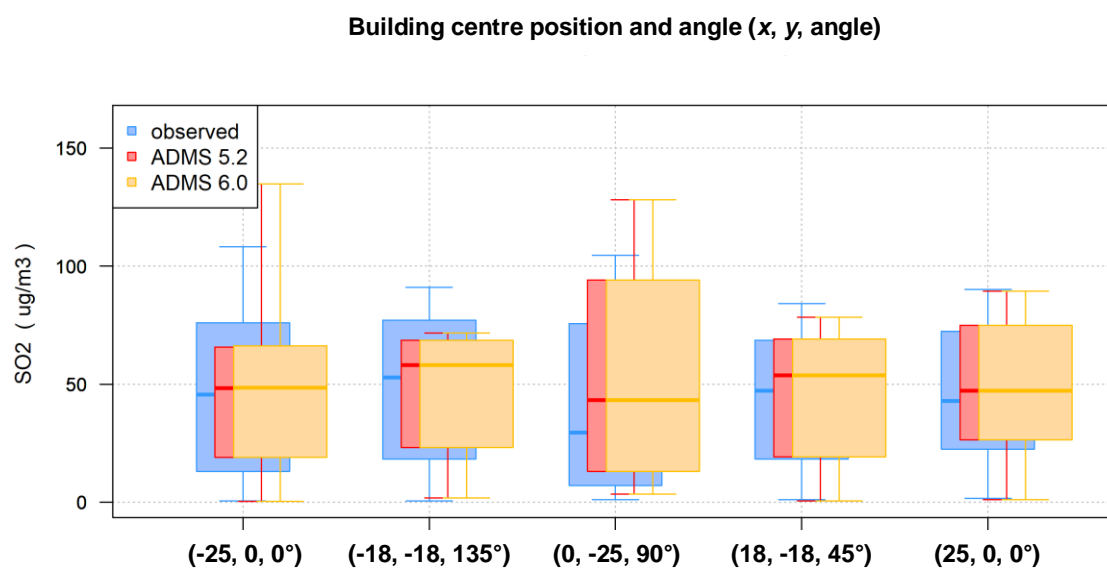


**Figure 6** – Box and whisker plot of model results, variation with building centre position and angle.

#### 4 Additional information: calculation of emission characteristics

Snyder considered a steam boiler with the characteristics as a base case shown in **Table 7**.

$l$ (m)	$w$ (m)	$H_b$ (m)	$L$ (m)	$D_s$ (m)	$H_s$ (m)	$W_s$ (m/s)	$T_s$ (K)	$U_s$ (m/s)
100	40	50	25	6	75	20	418	13.4

**Table 7** – Parameters of the steam boiler for the base case (at full scale) with  $l$  the building length,  $w$  the building width,  $H_b$  the building height,  $L$  the distance from the building centre to the stack centre ( $L$  is positive if the stack is downstream of building),  $D_s$  the source diameter,  $H_s$  the source height,  $W_s$  the exit velocity,  $T_s$  the emission temperature, and  $U_s$  the wind speed at top of stack.

The parameters were formed into non-dimensional variables. The table below shows the base-case values, ranges of parameter variations, and number of values of each parameter tested in Snyder's original study.

	$H_s/H_b$	$L/H_b$	$\theta$ (°)	$W_s/U_s$	$Fr_a$	$\rho_s/\rho_a$
<b>Minimum</b>	0.25	-5.0	0	1.5	8	0.7
<b>Base</b>	1.50	0.5	0	1.5	16	0.7
<b>Maximum</b>	2.50	7.5	180	4.0	$\infty$	0.7

**Table 8** – Values of dimensionless groups used in Snyder's original study. The meaning of  $\theta$ ,  $Fr_a$ ,  $\rho_s$  and  $\rho_a$  is explained below; see caption of **Table 7** for meaning of the other variables.

In the wind tunnel experiments, a mixture of air and helium was used to simulate the full-scale high temperature emissions. For the model runs  $T_s$  was specified explicitly, giving the same ratio of source density to ambient (see below).

Here  $\theta$  is the building orientation (defined as zero when the wind direction is perpendicular to the long face of building).  $\rho_s$  and  $\rho_a$  are effluent and ambient density respectively.  $Fr_a$  is the



Froude number expressed as follows:

$$Fr_a = \frac{W_s^2}{gD_s(\Delta T/T_a)},$$

where  $T_a$  is the ambient temperature (in K) at the stack top,  $\Delta T = T_s - T_a$ .

For the base case  $Fr_a = 16$ ,  $W_s = 20$  m/s,  $D_s = 6$  m and  $T_s = 418$  K, substituting these values into the expression for the Froude number gives the ambient temperature  $T_a = 293$  K.

#### *Emission density*

For a perfect gas,

$$P = \frac{\rho RT}{M},$$

where  $P$  is pressure,  $\rho$  is the density,  $R = 8.314$  J kg<sup>-1</sup>mol<sup>-1</sup> is the universal gas constant,  $T$  is the absolute temperature and  $M$  is the molecular weight.

For a particular gas, at a fixed pressure this gives

$$\rho_1 T_1 = \rho_2 T_2.$$

Hence, if  $T_1 = 418$  K and  $T_2 = 293$  K,

$$\rho_1 = 0.7 \rho_2.$$

Hence for the model runs, the gas released may be assumed to have the properties of air (i.e.  $c_p = 1012$  J/kg<sup>-1</sup>K<sup>-1</sup>,  $M = 28.96$  g), with  $T_s = 418$  K (= 145°C) and  $T_a = 293$  K (= 20°C).

## 5 References

- [1] Snyder, W.H., 1993: *Downwash of Plumes in the Vicinity of Buildings – A Wind Tunnel Study*. In proceedings of the NATO Advanced Research Workshop: "Recent Research Advances in the Fluid Modeling Mechanics of Turbulent Jets and Plumes", Viano do Castelo, Portugal, June 28 - July 2, 1993.
- [2] Stidworthy A, Carruthers D, Stocker J, Balis D, Katragkou E, and Kukkonen J, 2013: *MyAir Toolkit for Model Evaluation*. 15<sup>th</sup> International Conference on Harmonisation, Madrid, Spain, May 2013.
- [3] Thunis P., E. Georgieva, S. Galmarini, 2010: *A procedure for air quality models benchmarking*. [https://fairmode.jrc.ec.europa.eu/document/fairmode/WG1/WG2\\_SG4\\_benchmarking\\_V2.pdf](https://fairmode.jrc.ec.europa.eu/document/fairmode/WG1/WG2_SG4_benchmarking_V2.pdf)
- [4] David Carslaw and Karl Ropkins (2011). *openair: Open-source tools for the analysis of air pollution data*. R package version 0.4-7. <http://www.openair-project.org/>
- [5] Chang, J. and Hanna, S., 2004: *Air quality model performance evaluation*. Meteorol. Atmos. Phys. **87**, 167-196.